



High Gain DC-DC Converter using Active Clamp Circuit

M. Prabhakar*

School of Electrical Engineering, VIT University, Chennai, India

PAPER INFO

Paper history:

Received 11 January 2013
Received in revised form 07 May 2013
Accepted 22 August 2013

Keywords:

DC-DC Converter
Resonant Power Conversion
Voltage Gain

ABSTRACT

In this paper, a boost converter with a clamp circuit is proposed for high intensity discharge (HID) lamp application. The clamp circuit provides zero voltage turn on for both main and clamp switches. Compared to conventional boost converters, the proposed converter has the following advantages: (i) high voltage gain without suffering from extreme duty ratio, (ii) low stress on the switches and (iii) low switching losses. Simulation and experimental results show that the voltage stress on the switches are well within acceptable limits and prove the converter's performance over a wide load range.

doi: 10.5829/idosi.ije.2014.27.01a.15

1. INTRODUCTION

Many applications like DC back up energy storage system for UPS, HID headlamps, medical equipments etc., driven by battery power source require high efficiency, high conversion ratio DC-DC converters. Conventional boost converters that are used to achieve high voltage gain employ various topologies and methods. One method of obtaining high voltage gain is increasing the duty cycle of the converter [1-4]. This gives rise to severe reverse recovery problems and leads to higher switch stress causing reduction in efficiency and EMI problems. Flyback topologies can be used; but, they impose severe voltage and current stress on the components due to the leakage inductance in the transformer windings [1, 5-9].

High voltage gain can also be obtained by paralleling the devices and circuits because of their advantages like expandability and reliability [3]. However, they suffer from interconnection complexity, unequal load sharing and current sharing problems. Hence, they cause system instability. Cascaded boost converters and quadratic converters are also employed to achieve high voltage gain without extreme duty cycle

[10, 11]. Nevertheless, they suffer from stability and synchronization problems and also high voltage stress.

Some circuit topologies utilizing coupled inductors may also be used for achieving high voltage gain [4, 8, 10]. The coupled inductor reduces the switch voltage stress. Thus, it eliminates the reverse recovery problems of the diode. However, the leakage energy in the coupled inductor results in high voltage ripple across the switch because the resonant effect leads to degraded power conversion efficiency. Therefore, it becomes necessary to protect the switch from the voltage ripples. This can be achieved by using an active snubber circuit or high voltage rated device with sufficiently high R_{DS} to deplete the leakage energy of the inductor. In addition, this topology may result in input current pulsations and require filtering. Switched capacitors can be utilized to obtain high voltage gain based upon the number of capacitors used in the circuit [11, 12]. For low power applications, they provide high power density, high efficiency, good stability and reduced EMI problems due to the absence of magnetic devices. Nevertheless, their efficiency decreases when a constant output voltage is required. They cannot provide voltage regulation for variations in the line voltage due to relatively high output voltage ripples.

Active clamp circuits can also be employed to achieve high voltage gain with reduced switch stress

*Corresponding Author Email: prabhakar.m@vit.ac.in (M. Prabhakar)

since they effectively recycle the transformer’s leakage energy [1, 13]. However, the voltage gain is about 5 in [14]. This is not suitable for the HID lamp application which requires a voltage gain of 10 when fed from a 12V battery source. In this paper, an active clamp circuit based boost converter is presented for a HID headlamp application. Unlike the existing converter, the proposed converter is designed to work over a wide load range from 35W to 350W. The circuit configuration, modes of operations, steady state analysis, design specifications, simulation and hardware results are presented in this paper.

2. CIRCUIT DESCRIPTION

The voltage conversion ratio of a conventional boost converter is given by

$$\frac{V_o}{V_m} = \frac{1}{1-D} \tag{1}$$

where, D is the duty cycle. When a gain of more than 5 is required, conventional boost converters are not suitable due to restriction on duty cycle and reverse recovery problems. In case of cascaded boost converter, the gain is given by

$$\frac{V_o}{V_m} = \frac{1}{(1-D)^2} \tag{2}$$

Thus, high voltage gain can be achieved without suffering from extreme duty ratio. However, circuit becomes complex as more components need to be used. Figure 1 shows a boost converter which is used to overcome the drawbacks of a cascaded boost converter. Here, the power switch is operated in hard switching which results in increased switching losses.

To reduce the switching losses of the power switch, soft switching is achieved using an active clamp circuit as shown in Figure 2. The active clamp circuit consists of a switch Q_a , clamp capacitor C_c and a resonant inductor L_r which resonate with the body capacitance C_r of the main switch Q to achieve ZVS of both the switches.

The main switch and the clamp switch operate in complementary fashion with a short resonant time delay. When the main switch is turned off, the inductor current i_{Lr} flows through the body diode of the clamp switch, the clamp capacitor and to the ground. This forces the drain to source voltage of the clamp switch to fall zero. Hence, it can be turned on to achieve soft switching. Similarly, when the clamp switch is off, the negative inductor current i_{Lr} flows through the resonant capacitor which discharges and reaches zero so as to achieve ZVS of the main switch.

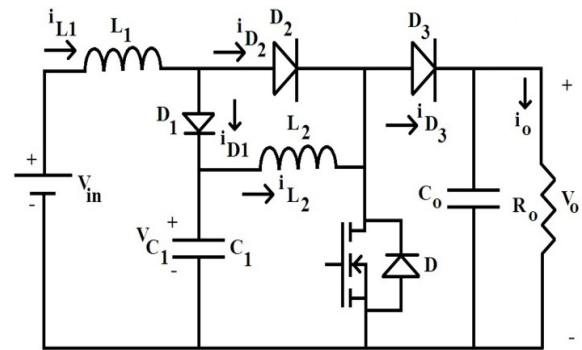


Figure 1. Power circuit of hard switched cascaded boost converter

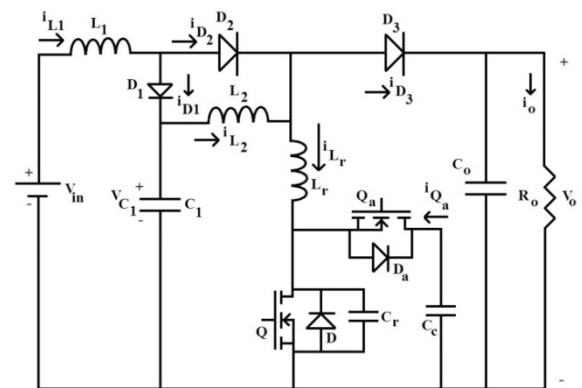


Figure 2. Power circuit of the cascaded boost converter with active clamp circuit

3. MODES OF OPERATION

The following assumptions are made to explain the modes of operation of the proposed circuit:

- i. The values of capacitors C_1 , C_c , C_0 are kept large enough such that the voltage across them is maintained constant.
- ii. The energy stored in the resonant inductor L_r is greater than the energy stored in the resonant capacitor C_r , this ensures soft switching of both main and clamp switch.
- iii. The inductances L_1 and L_2 are greater than the inductance of L_r .

Figure 3 shows the characteristic waveforms of the circuit operating under continuous conduction mode (CCM) for one switching cycle.

3. 1. Mode 1 [$t_0 < t < t_1$] In this mode, the main switch Q is turned on, the clamp switch Q_a is off. The diodes D_1 and D_3 are off and D_2 is in conduction. The capacitor C_0 discharges to feed the load. Since L_1 and L_2 is greater than L_r , the inductor currents i_{L1} and i_{L2} increases which is given by the governing equations as given below

$$i_{L1} = i_{L1}(t_0) + \frac{V_{in}DT}{L_1} \tag{3}$$

$$i_{L2} = i_{L2}(t_0) + \frac{V_{C1}DT}{L_2} \tag{4}$$

where, D is the duty cycle of the main switch. The switch currents are given by $i_Q = I_{Lr}$ and $i_{Qa} = 0$. The inductor voltages are given by

$$V_{L1} + V_{Lr} = V_{in} \tag{5}$$

$$V_{L2} + V_{Lr} = V_{C1} \tag{6}$$

3. 2. Mode 2 [$t_1 < t < t_2$] The main switch Q is turned off at t_1 . D_2 is still conducting. The positive inductor current i_{Lr} charges the resonant capacitor C_r . Since C_r is very small, it is charged linearly and is given by the following equation:

$$V_{Cr} = \frac{i_{Lr}(t_1)(t - t_1)}{C_r} \tag{7}$$

As long as $V_{Cr} < V_{C1}$, the diodes D_1 and D_3 remain in reverse bias. When $V_{Cr} = V_{C1}$, voltage across D_1 and C_1 is approximately equal to V_{C1} . Therefore, D_1 is turned on. Now, the diode current i_{D1} increases and i_{D2} decreases. C_r charges further till it is equal to V_{Cc} . When $V_{Cr} = V_{Cc}$, the antiparallel diode of clamp switch is turned on. This forces the drain to source voltage of the clamp switch to zero. The switch can now be turned on to realize ZVS. This mode ends when $i_{D2} = 0$ and D_3 is turned on.

3. 3. Mode 3 [$t_2 < t < t_3$] This mode begins when D_3 is turned on at t_2 . The inductor currents i_{L1} and i_{L2} decrease which in turn decreases i_{Lr} . i_{Lr} decreases from positive value to zero and then goes to negative value. Before i_{Lr} becomes negative, Q_a is turned off. This mode ends when Q_a is turned off at t_3 . The inductor current is given by

$$i_{Lr}(t) = i_{Lr}(t_2) - \frac{(V_{Cc} - V_0)(t - t_2)}{L_r} \tag{8}$$

3. 4. Mode 4 [$t_3 < t < t_4$] In this mode, D_3 remains in conduction. The negative inductor current i_{Lr} discharges the capacitor C_r . The capacitor voltage V_{Cr} decreases from V_{Cc} to zero. When $V_{Cr} = 0$, the antiparallel diode of the main switch is turned on. This makes the drain to source voltage of the main switch equal to zero. The main switch Q can now be turned on at this instant to achieve ZVS. This mode ends when Q is turned on. The output diode currents i_{D3} decreases. When $i_{D3} = 0$, D_2 is turned on.

3. 5. Mode 5 [$t_4 < t < t_5$] This mode commences when D_3 is turned off and D_1 and D_2 are in commutation interval. The voltage across inductor L_2 is zero. Hence, $V_{C1} = V_{Lr}$ thereby increasing i_{Lr} . The diode currents i_{D1} decreases and i_{D2} increases. This mode ends when $i_{D1} = 0$, so it turns off D_1 .

4. STEADY STATE ANALYSIS

Applying voltage-second balance across inductances L_1 and L_2 and neglecting the duty cycle losses for each mode, we can obtain the steady state voltage gain of the circuit. When the switch Q is closed, $V_{L1} = V_{in}$ and $V_{L2} = V_{C1}$. When the switch is open, $V_{L1} = V_{in} - V_{C1}$ and $V_{L2} = V_{C1} - V_0$. Thus, we have

$$V_{in}D + (v_{in} - V_{C1})(1 - D) = 0 \tag{9}$$

Rearranging Equation (9), we get a gain which is given by Equation (10).

$$\frac{V_{C1}}{V_{in}} = \frac{1}{1 - D} \tag{10}$$

Similarly, applying volt-second balance for the inductor L_2 , we get,

$$V_{C1}D + (V_{C1} - V_0)(1 - D) = 0 \tag{11}$$

Rearranging Equation (11) yields,

$$\frac{V_0}{V_{C1}} = \frac{1}{1 - D} \tag{12}$$

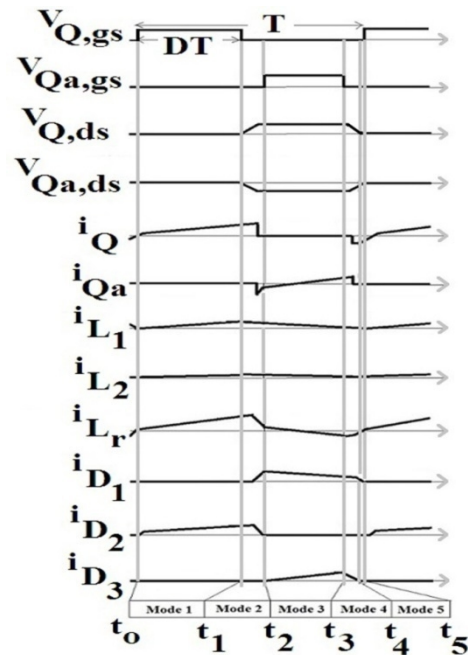


Figure 3. Characteristic waveforms of the proposed circuit

Combining Equations (10) and (12), we get the overall conversion ratio as

$$M = \frac{V_o}{V_{in}} = \frac{1}{(1-D)^2} \quad (13)$$

5. DESIGN SPECIFICATIONS

The efficiency of the given circuit is given by

$$\eta = \frac{P_o}{i_{L1,av} V_{in}} \quad (14)$$

The maximum duty cycle of the main switch is obtained at minimum input voltage and is expressed as

$$D_{max} = 1 - \sqrt{\frac{V_{in,min}}{V_o}} \quad (15)$$

If the ripple currents Δi_{L1} and Δi_{L2} are given, the value of inductances L_1 and L_2 can be obtained as follows

$$L_1 > \frac{DTV_{in}}{\Delta i_{L1}} \quad (16)$$

$$L_2 > \frac{DTV_{in}}{\Delta i_{L2}(1-D)} \quad (17)$$

The energy stored in the resonant inductor L_r should be greater than the energy stored in the resonant capacitor C_r to achieve soft switching of both the main and the clamp switches. This assumption can be used to calculate the value of L_r or C_r if one of the values is known.

$$L_r > \frac{C_r V_{C_c}^2}{(i_{L_r}(t_s))^2} \quad (18)$$

The delay time between the main switch and the clamp switch is given by $\pi\sqrt{L_r C_r}/2$. If C_r is known, the value of L_r can be obtained by the following equation

$$L_r \cong \frac{4t_d^2}{\pi^2 C_r} \quad (19)$$

In addition, half the resonant period is larger than the off time of the main switch Q . Therefore, we get the Equation (20) for C_c as follows

$$C_c = \frac{(1-D)^2 T^2}{L_r \pi^2} \quad (20)$$

Using the Equations (14) to (20), the values of L_r , C_r , C_c , L_1 , L_2 and D are obtained. Based on the voltage ripple, the output capacitor C_o is computed using Equation (21).

$$C_o = \frac{V_{in} D}{2R_o \Delta V} \quad (21)$$

6. SIMULATION RESULTS

The proposed circuit with the specifications given in Table 1 was simulated using Pspice. Figure 4 shows the output voltage and output power waveforms for the load equivalent to 120V, 35W. Figure 5 shows the gate voltage, drain to source voltage and switch current of the main switch Q . Here, the switch can be turned on when the drain to source voltage of the switch is approximately zero. This ensures ZVS of the main switch Q . Figure 6 shows the gate and drain voltages and current through the clamp switch Q_a . Before the switch is turned on, the current through the switch is negative and the voltage across it is near zero as soft switching also achieve for the clamp switch. From Figures 5 and 6, it is observed that the stress across the switches is found to be 100V which is less than the output voltage.

TABLE 1. Specifications of the proposed circuit

Parameter	Value
Input voltage	12V
Output Voltage	120V
Output Power	35W – 350W
Switching frequency	50kHz
L_1	500 μ H
L_2	4mH
Resonant Inductor L_r	15 μ H
Capacitors C_1	220 μ F
Resonant Capacitor C_r	600pF
Clamp Capacitor C_c	800nF
Output Capacitor C_o	20mF
Switches Q and Q_a	IRF740 (400V, 10A, 0.55 Ω)
Diodes D_1 , D_2 and D_3	MUR860 (200V, 8A)

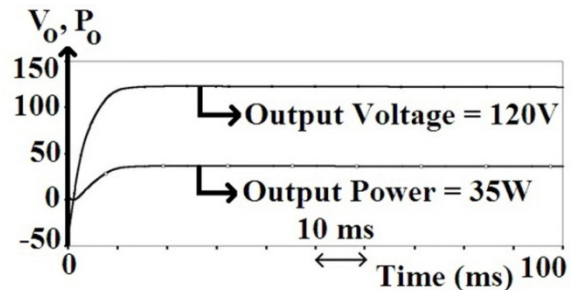


Figure 4. Output voltage and output power plots

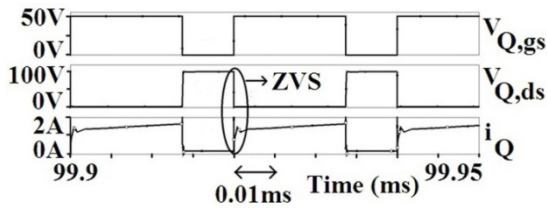


Figure 5. Gate voltage $V_{Q,gs}$, Drain to Source voltage $V_{Q,ds}$ and Current i_Q through the main switch Q.

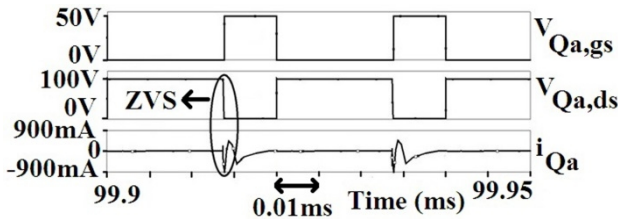


Figure 6. Gate voltage $V_{Qa,gs}$, Drain to Source voltage $V_{Qa,ds}$ and Current i_{Qa} through then clamp switch Q_a .

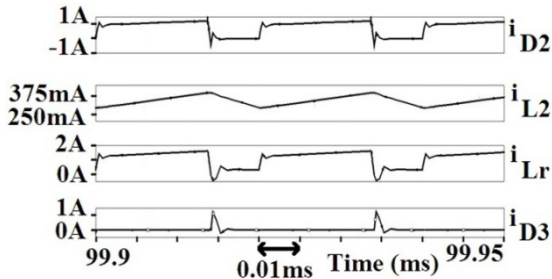


Figure 7. Plot of i_{D2} , i_{L2} , i_{Lr} and i_{D3} .

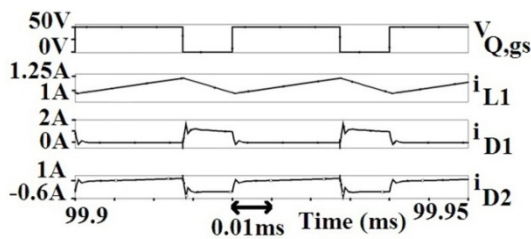


Figure 8. Gate voltage $V_{Q,gs}$ of main switch Q, currents i_{L1} , i_{D1} and i_{D2} .

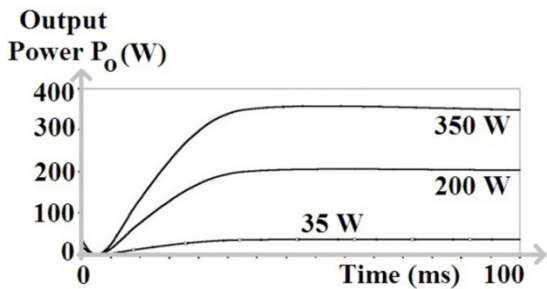


Figure 9. Power plots for various load conditions

Figure 7 shows the plot of currents through various circuit elements. From the graph, it is inferred that the algebraic sum of currents through D_2 and L_2 equals the algebraic sum of currents through D_3 and L_r . Figure 8 shows the impact of the gate voltage of the main switch Q on various currents in the circuit. When the gate voltage is present, the inductor is charged and gets discharged when the gate pulse is turned off. The currents through the diodes D_1 and D_2 are complementary to each other. When the gate pulse is present, the current i_{D2} increases and i_{D1} is zero and vice versa when gate pulse is absent. Though the power rating of HID lamp is 35W, the converter's performance was tested till 350W. The results prove that the converter provides the required voltage gain and meets the power requirement as shown in Figure 9.

7. EXPERIMENTAL RESULTS

The experimental set up of the proposed converter with the specifications mentioned in Table 1 was built and tested for verifying its performance. Figure 10 shows the gate pulses applied to the main and auxiliary switches. The converter duty cycle, complementary nature of the gate pulses and the voltage across the switches can be verified from Figure 10. The application and removal of gate pulse to the main switch causes energy storage and dissipation across the inductor, respectively. This behaviour of the proposed converter is verified from Figure 11. The proposed converter provided the required voltage gain of 10. As a result, the output voltage was 123 V which closely matches with the theoretical design and simulation results. Further, based on the output current waveform, it can be verified that the output power obtained at the output was 320W which explains the operating range of the proposed converter. Figure 12 confirms the wide operating range of the proposed converter along with its ability to provide the required output voltage and output current. The voltage stress across the main and auxiliary switches is within acceptable limits and is shown in Figures 13 and 14, respectively.

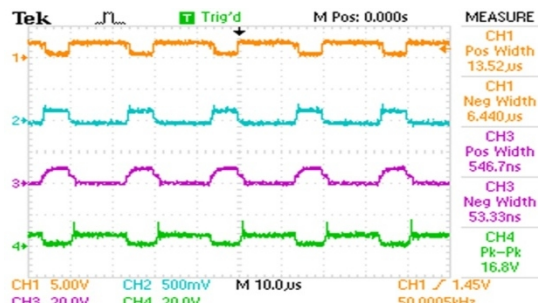


Figure 10. Gate pulse and voltage across main and auxiliary switches

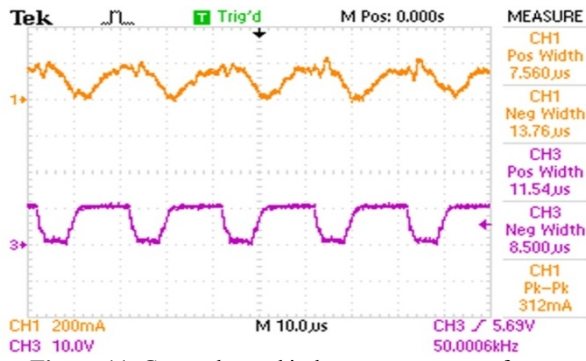


Figure 11. Gate pulse and inductor current waveforms

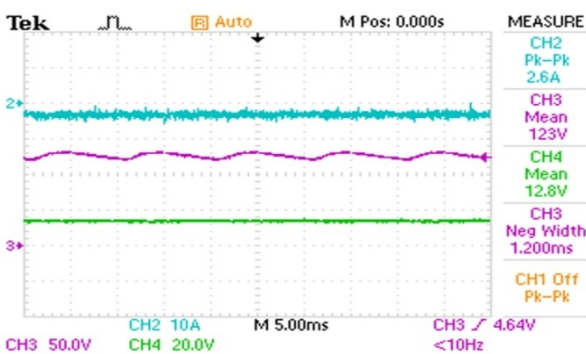


Figure 12. Input voltage, output voltage and output current waveforms

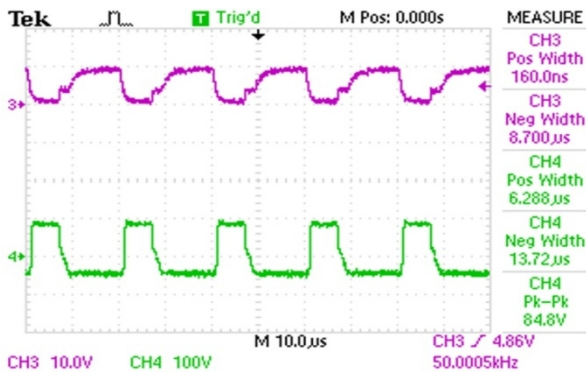


Figure 13. Gate pulse and voltage across main switch

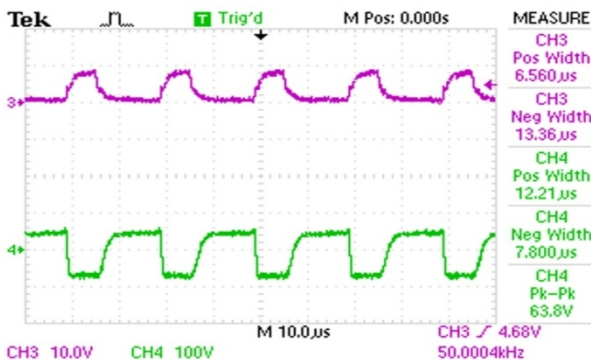


Figure 14. Gate pulse and voltage across auxiliary switch

8. CONCLUSION

The operational details, analysis and experimental results of a high gain DC-DC converter with clamp circuit have been presented in this paper. By addition of resonant elements L_r and C_r , soft switching of both the main and auxiliary switches has been achieved. Experimental results obtained from the proposed circuit prove that the converter operates under ZVS condition over a wide load range. Further, the converter is capable of providing the required voltage gain of 10 and delivers the required load power. In addition, the voltage stress across the switches is within acceptable limits due to soft switching of the main and auxiliary switches.

9. REFERENCES

- Liang, T.-J. and Tseng, K., "Analysis of integrated boost-flyback step-up converter", in *Electric Power Applications*, IEE Proceedings-, IET. Vol. 152, (2005), 217-225.
- Klimeczak, P. and Munk-Nielsen, S., "Comparative study on paralleled vs. Scaled DC-DC converters in high voltage gain applications", in *Power Electronics and Motion Control Conference*, EPE-PEMC. 13th, IEEE. (2008), 108-113.
- Wai, R.-J. and Duan, R.-Y., "High step-up converter with coupled-inductor", *Power Electronics, IEEE Transactions on*, Vol. 20, No. 5, (2005), 1025-1035.
- Zhao, Q. and Lee, F. C., "High-efficiency, high step-up DC-DC converters", *Power Electronics, IEEE Transactions on*, Vol. 18, No. 1, (2003), 65-73.
- Alcazar, Y. J. A., Bascopé, R. T., de Oliveira, D., Andrade, E. H. and Cárdenas, W. G., "High voltage gain boost converter based on three-state switching cell and voltage multipliers", in *Industrial Electronics*, 34th Annual Conference of IEEE, (2008), 2346-2352.
- Araujo, S. V., Torrico-Bascope, R. P. and Torrico-Bascope, G. V., "Highly efficient high step-up converter for fuel-cell power processing based on three-state commutation cell", *Industrial Electronics, IEEE Transactions on*, Vol. 57, No. 6, (2010), 1987-1997.
- Tsai, C.-T. and Shen, C.-L., "Interleaved soft-switching buck converter with coupled inductors", in *Sustainable Energy Technologies*, International Conference on, IEEE. (2008), 877-882.
- Tseng, K. and Liang, T.-J., "Novel high-efficiency step-up converter", *IEE Proceedings-Electric Power Applications*, Vol. 151, No. 2, (2004), 182-190.
- Zhao, Q., Tao, F., Hu, Y. and Lee, F. C., "Active-clamp DC/DC converters using magnetic switches", in *Applied Power Electronics Conference and Exposition*, Sixteenth Annual IEEE, Vol. 2, (2001), 946-952.
- Reatti, A., "Low-cost high power-density electronic ballast for automotive hid lamp", *Power Electronics, IEEE Transactions on*, Vol. 15, No. 2, (2000), 361-368.
- Mak, O.-C., Wong, Y.-C. and Ioinovici, A., "Step-up DC power supply based on a switched-capacitor circuit", *Industrial Electronics, IEEE Transactions on*, Vol. 42, No. 1, (1995), 90-97.
- Abutbul, O., Gherlitz, A., Berkovich, Y. and Ioinovici, A., "Step-up switching-mode converter with high voltage gain using

- a switched-capacitor circuit", ***Circuits and Systems I: Fundamental Theory and Applications, IEEE Transactions on***, Vol. 50, No. 8, (2003), 1098-1102.
13. Ismail, E. H., Al-Saffar, M. A. and Sabzali, A. J., "High conversion ratio DC-DC converters with reduced switch stress", ***Circuits and Systems I: Regular Papers, IEEE Transactions on***, Vol. 55, No. 7, (2008), 2139-2151.
14. Lin, B.-R. and Chen, J.-J., "Analysis and implementation of a soft switching converter with high-voltage conversion ratio", ***Power Electronics, IET***, Vol. 1, No. 3, (2008), 386-394.

High Gain DC-DC Converter using Active Clamp Circuit

RESEARCH NOTE

M. Prabhakar

School of Electrical Engineering, VIT University, Chennai. India

PAPER INFO

چکیده

Paper history:

Received 11 January 2013

Received in revised form 07 May 2013

Accepted 22 August 2013

Keywords:

DC-DC Converter

Resonant Power Conversion

Voltage Gain

در این مقاله، یک تبدیل کننده بوستر (تقویت کننده) با مدار بسته برای کاربرد در لامپ تخلیه شدت بالا پیشنهاد شده است. مدار بسته که ولتاژ صفر را ایجاد می کند برای کلیدهای اصلی و بسته روشن می شود. در مقایسه با تبدیل کننده های رایج بوستر، تبدیل کننده پیشنهادی فواید زیر را دارد: (i) بهره ولتاژ بالا بدون مزاحمت نسبت بار نهایی، (ii) فشار پایین روی کلیدها و (iii) اتلافات کم در هنگام کلیدزدن. نتایج شبیه سازی و تجربی نشان می دهد که فشار ولتاژ روی کلیدها در محدوده قابل قبول است و عملکرد تبدیل کننده را در دامنه گسترده بارگذاری اثبات می کند.

doi: 10.5829/idosi.ije.2014.27.01a.15.
